ELSEVIER

Short-step syntheses and complexation properties of Z,Z-tribenzodidehydro- and *all-Z*-tribenzo[12]annulenes

Siriwan Sirinintasak, Yoshiyuki Kuwatani, Shin-ichi Hoshi, Eigo Isomura, Tohru Nishinaga and Masahiko Iyoda*

Department of Chemistry, Graduate School of Science and Engineering, Tokyo Metropolitan University, Hachioji, Tokyo 192-0397, Japan

Abstract—Syntheses of *all-Z*-tribenzo[12]annulenes (**1a–c**) and Z,Z-tribenzodidehydro[12]annulenes (**2a–c**) by the reduction of the corresponding tribenzohexadehydro[12]annulenes **3a–c** were carried out using a low valent titanium complex generated from Ti(O-*i*-Pr)$_4$ and *i*-PrMgCl. The unique structure of the first reduction products **2a–c** as well as **1a–c** was fully characterized. Complexation of these annulenes with silver(I) ions produces the corresponding silver complexes. Among them, the silver complexes of **2a–c** exhibit interesting monomer–dimer equilibrium.
© 2007 Elsevier Ltd. All rights reserved.

Bowl-shaped cyclophanes play an important role in the supramolecular chemistry, because they can act as a host molecule for incorporation of guest molecules or ions using the electron rich cavity surrounded by aromatic rings.[1] They also form inclusion crystals which accommodate small molecules in the crystal lattice. Furthermore, they can be used as a component of designed artificial large host molecules for more efficient and practical applications in the molecular recognition, sensing, and catalysis. In this context, *all-Z*-tribenzo-[12]annulene **1a** is an interesting candidate for the novel host molecules.[2] This compound forms a stable 1:1 metal complex with Ag(I) or Cu(I) ion by the use of 'pre-

organized' three double bonds.[2c] We have been interested in this compound and investigated its synthetic pathways.[3] To develop new π-cavitands based on this structure, a new synthetic strategy has been investigated. The basic strategy reported here is the reduction of three triple bonds in tribenzohexadehydro[12]annulene **3a**, which is an easily accessible compound.[4]

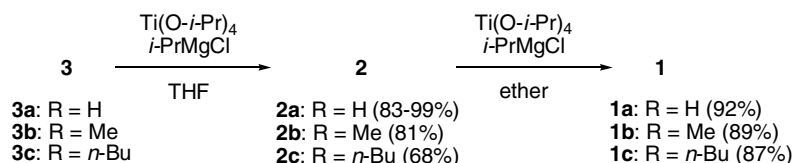Although the reduction of **3a** with the standard Lindlar catalyst was studied by Staab et al. to produce the corresponding Z,Z-dieneyne **2a** and E,Z,Z-tribenzo[12]-annulene,[5] the structure and properties of **2a** was not fully investigated, presumably due to low selectivity of
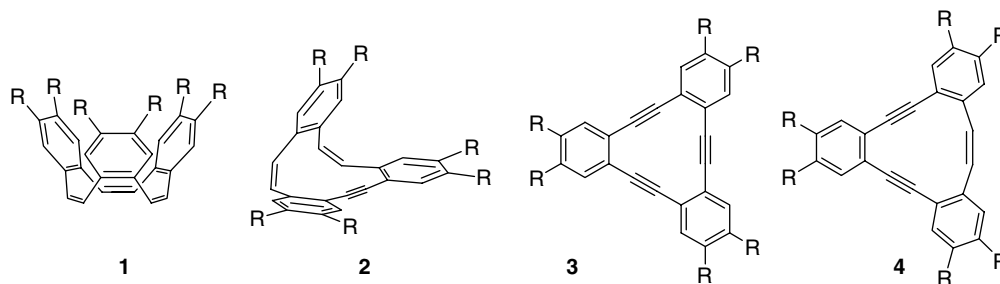
**a**: R = H, **b**: R = Me, **c**: R = *n*-Bu

Scheme 1. Synthesis of **2** and **1** by the reduction of benzodehydroannulenes **3**.

the reduction. To develop a selective and effective method for the conversion of **3a–c** into **1a–c** via **2a–c**, the reduction of **3a–c** was examined using a low valent titanium complex generated from Ti(O-*i*-Pr)$_4$ and *i*-PrMgCl[6] (Scheme 1).

Reduction of **3a–c** with low valent titanium complex using a large excess of reagents yielded **2a–c** selectively.[7] Thus, the reaction of **3a** with Ti(O-*i*-Pr)$_4$ (50 equiv) and *i*-PrMgCl (100 equiv) in THF at −50 °C for 2 h or Ti(O-*i*-Pr)$_4$ (10 equiv) and *i*-PrMgCl (20 equiv) in THF at 0 °C for 2 h produced **2a** in 99% or 83% yield, respectively.[8] The reduction of hexamethyl derivative **3b** proceeded smoothly under the similar reaction conditions, and the reaction of **3b** with Ti(O-*i*-Pr)$_4$ (10 equiv) and *i*-PrMgCl (20 equiv) in THF at 0 °C for 2 h gave **2b** in 81% yield. The reduction of the hexabutyl derivative **3c** also produced the corresponding reduction product **2c** in 68% yield under the similar conditions.[8]

Further reduction of **2a–c** also proceeded smoothly to give *all-Z*-tribenzo[12]annulenes **1a–c**. Thus, the reaction of **2a** with Ti(O-*i*-Pr)$_4$ (5 equiv) and *i*-PrMgCl (10 equiv) in ether at −50 °C for 1 h afforded **1a** in 92% yield. The similar reaction of methyl derivative **2b** was relatively slow at −50 °C probably due to its low solubility under the reaction conditions and gave the corresponding reduction product **1b** in lower yield (68%). However, the reaction at 0 °C for 1 h gave **1b** in 89% yield. The similar reduction of more soluble **2c** at −50 °C for 1 h gave **1c** in 87% yield. It is worth noting that direct reduction of **3a–c** to **1a–c** was not successful possibly due to steric reasons for multiply titanium-coordinated intermediate.

To examine the applicability of the same reduction for the synthesis of **1a** and **2a** from *Z*-tribenzotetradehydro[12]-annulene **4a**,[9] the reduction of **4a** with low valent titanium reagent was performed. Although the reaction of **4a** with Ti(O-*i*-Pr)$_4$ (3 equiv) and *i*-PrMgCl (6 equiv) in THF at 0 °C for 2 h gave a 4:6 mixture of **1a** and **2a** in totally 80% yield, similar reaction of **4a** with Ti(O-*i*-Pr)$_4$ (5 equiv) and *i*-PrMgCl (10 equiv) in ether at −50 °C for 1 h selectively produced **2a** in 92% yield.
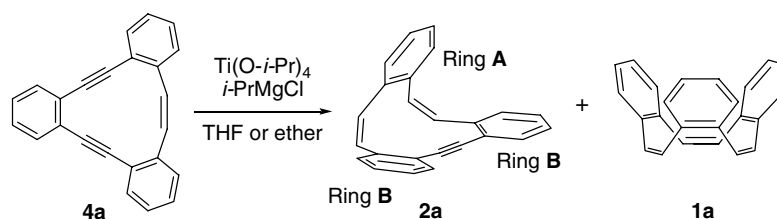
Benzannulenes **2a–c** are considered to behave as a folded *Cs* symmetric structure. ^{1}H NMR spectra of **2a–c** show characteristic signals for the aromatic protons of benzene ring **A** (see Scheme 2) in a high field. Thus, the two aromatic protons of **2a** were observed at δ 6.89–6.86 and 6.74–6.72 as AA′BB′ multiplets. The corresponding signals of **2b** and **2c** were observed at δ 6.50 and 6.48, respectively. These high field shifts of the aromatic protons of ring **A** suggest that the protons locate in the shielding region of benzene ring **B** in the diphenylacetylene moiety.

The molecular and crystal structures of **2a** and **2b** were unambiguously determined by X-ray crystallographic analysis.[10,11] As shown in Figure 1, the diphenylacetylene moiety in **2a** shows a highly planar structure. The maximum atomic deviation from the least-squares plane defined by the 14 carbon atoms of **2a** is 0.04 Å. The molecular structure is totally V-shaped arrangement of the diphenylacetylene moiety and benzene ring **A** with a dihedral angle of 62°. This molecular structure is in good accordance with the higher field shift of benzene ring **A** (δ 6.72–6.74 and 6.86–6.89) in the ^{1}H NMR spectrum. The molecule forms a dimeric structure by the stacking of the diphenylacetylene moiety with a distance of 3.4 Å in the crystal (Fig. 1b and c).

As reported previously, the unique structure of *all-Z*-tribenzo[12]annulene **1a** was proved to be suitable for the metal complexation with Ag(I).[3] The substituted analogs **1b** and **1c** also formed stable Ag(I) complexes by the reaction with silver salts. The coordination to the silver ion occurred at the three double bonds, which were clearly shown by the lower field shift of the olefinic protons (Δδ = 0.7–0.8 ppm) without significant changes for other signals.

Since didehydroannulenes (**2a–c**) possess a π-cavity composed of a triple bond and two double bonds, **2a–c** can be expected to behave as a π-cavitand. Actually, **2a–c** formed silver complexes with AgOTf, AgClO$_4$, and AgOCOCF$_3$. In the presence of AgOTf in CDCl$_3$, **2a** formed **2a**·AgOTf in which a triple bond and two double bonds can be expected to coordinate Ag(I) ion.

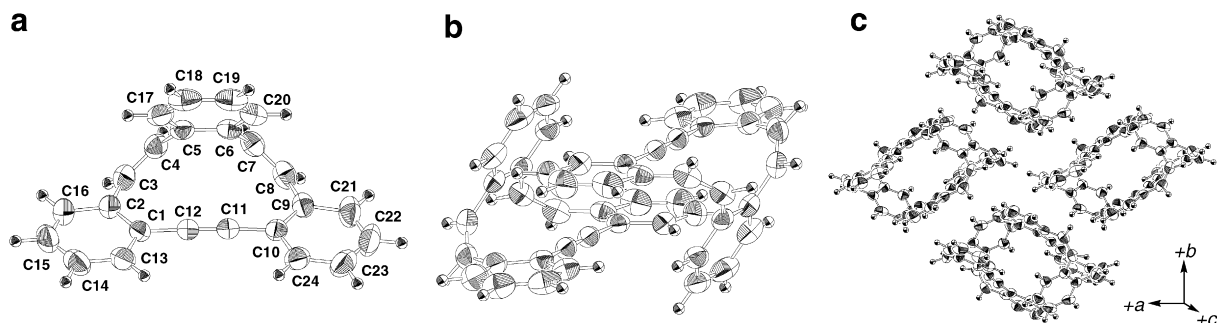**Scheme 2.** Reduction of **4a** by Ti(O-*i*-Pr)$_4$ and *i*-PrMgCl.

Figure 1. ORTEP drawing of **2a**. (a) Top view, (b) dimeric structure in the crystal, and (c) packing diagram. The selected bond lengths (Å) are as follows: C(1)–C(2) 1.404(2); C(2)–C(3) 1.473(2); C(3)–C(4) 1.326(2); C(4)–C(5) 1.478(2); C(10)–C(11) 1.437(2); C(11)–C(12) 1.191(2).

The ^{1}H NMR spectrum of **2a**·AgOTf in CDCl$_3$ at room temperature showed the olefinic protons at δ 7.72 and 7.12. Thus, the olefinic protons of **2a** (δ 7.10 and 6.79) were observed in a lower field, indicating the deshielding effect of Ag(I) ion. Interestingly, the ^{1}H NMR spectrum of **2a**·AgOTf in CDCl$_3$ is temperature dependent (Fig. 2). The olefinic proton Ha and the protons Hc–f of ring **B** in the diphenylacetylene moiety show a marked upper-field shift at low temperatures, whereas the olefinic proton Hb and the protons of ring **A** show small upper-field or lower-field shifts at low temperatures. We expected that the dimerization of **2a**·AgOTf takes place in CDCl$_3$ at low temperature. In a similar manner, the ^{1}H NMR spectra of the silver complexes **2b**·AgOTf and **2c**·AgOTf are temperature dependent. The VT-^{1}H NMR spectra of **2b**·AgOTf and **2c**·AgOTf also indicate the formation of a dimeric species, in which the benzene rings located in a face-to-face manner cause the signals at a high field (δ 6.0–6.5).

X-ray analyses of **2a**·AgClO$_4$[12] and **2a**·AgOTf[13] explain the temperature dependent NMR spectra of **2a**·AgOTf (Fig. 2). As shown in Figure 3, **2a**·AgClO$_4$ forms a sandwich-type complex in the crystal. Because of a shallow cavity and flat bottom structure of **2a** free from repulsive
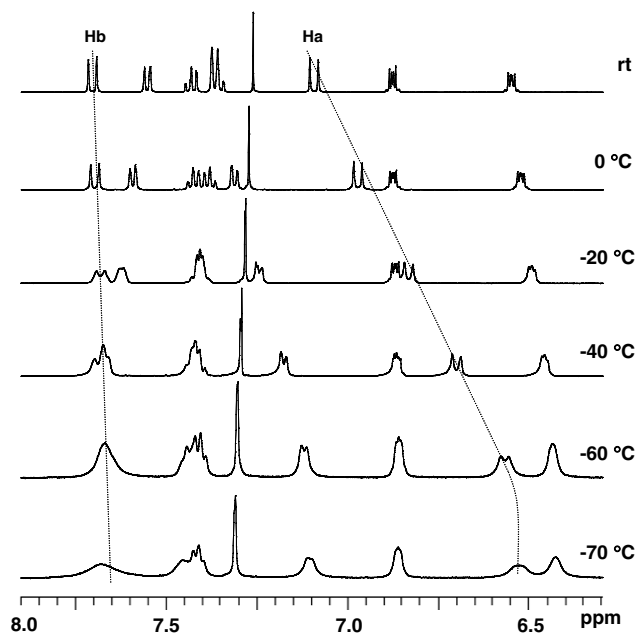
interaction between two ligands in the sandwich structure, **2a**·AgClO$_4$ can form a dimeric complex. Although the concentration of the dimer (**2a**·AgOTf)$_2$ is low at room temperature, the ratio of the dimer is increased at low temperatures, and only the dimer (**2a**·AgOTf)$_2$ exists in solution below −60 °C (Fig. 2).

In the case of **2c**·AgOTf, the monomer-dimer equilibrium occurs in CDCl$_3$ above −20 °C, whereas only the
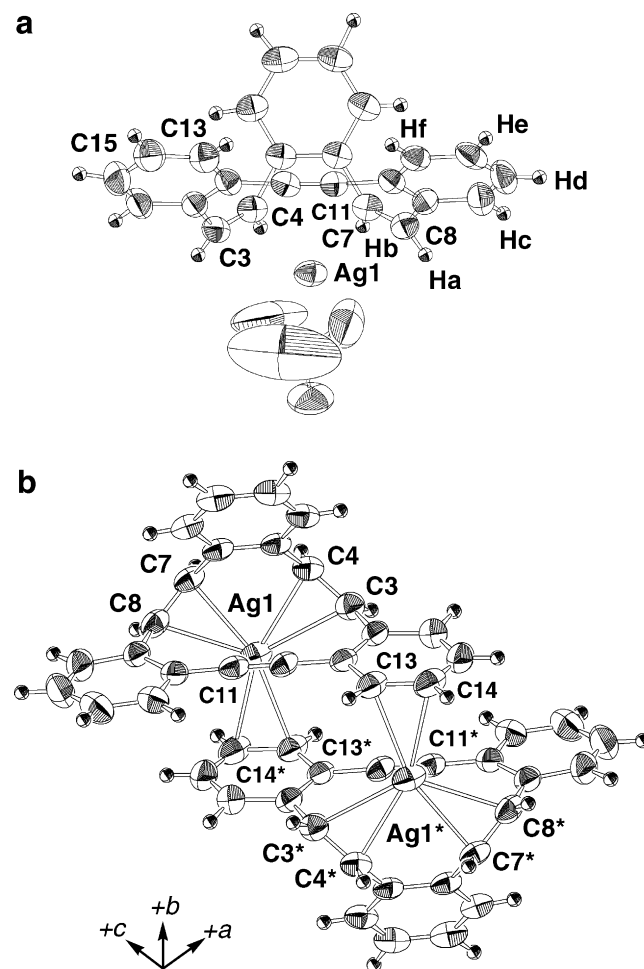

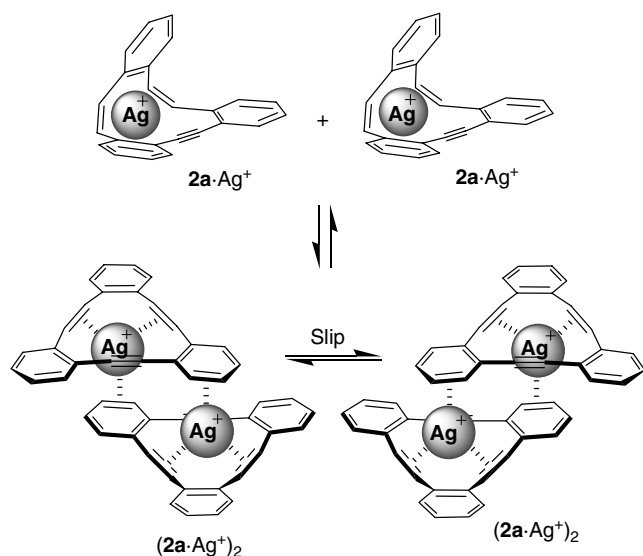**Figure 2.** VT ^{1}H NMR of **2a**·AgOTf in CDCl$_3$.

Figure 3. (a) ORTEP drawing of **2a**·AgClO$_4$. (b) Dimeric structure of **2a**·AgClO$_4$ (perchlorate ions are omitted for clarity). Selected bond distances (Å) are as follows: Ag(1)–C(3), 2.640(6); Ag(1)–C(4), 2.496(5); Ag(1)–C(7), 2.490(5); Ag(1)–C(8), 2.619(5); Ag(1)–C(11), 2.912(6); Ag(1)–C(13)*, 2.502(5); Ag(1)–C(14)*, 2.458(6).

Scheme 3. Monomer–dimer equilibrium in the silver complex of **2**.

dimer $(2c\cdot AgOTf)_2$ exists in solution below $-40\ ^\circ C$.[14] Because the symmetry of the spectrum does not change at low temperatures, the exchange process which includes dominantly intramolecular slipping is considered to be still fast (Scheme 3).

Supplementary data

Supplementary data associated with this article can be found, in the online version, at doi:10.1016/j.tetlet.2007.03.044.

References and notes

1. (a) Kawase, T.; Kurata, H. *Chem. Rev.* **2006**, *106*, 5250; (b) Tahara, T.; Tobe, Y. *Chem. Rev.* **2006**, *106*, 5274; (c) *Modern Cyclophane Chemistry*; Gleiter, R., Hopf, H., Eds.; Wiley-VCH: Weinheim, 2004; (d) Weber, E., Ed.; *Top. Curr. Chem.* **1994**, 172; (e) Vögtle, F. *Cyclophane Chemistry*; Wiley: New York, 1993; (f) Diederich, F. Cyclophanes. In *Monographs in Supramolecular Chemistry*; The Royal Society of Chemistry: London, 1991.
2. (a) Iyoda, M.; Kuwatani, Y.; Yamauchi, T.; Oda, M. *J. Chem. Soc., Chem. Commun.* **1989**, 65; (b) Mohler, D. L.; Vollhardt, K. P. C.; Stefan, W. *Angew. Chem., Int. Ed.* **1990**, *29*, 1151; (c) Kuwatani, Y.; Yoshida, T.; Kusaka, A.; Iyoda, M. *Tetrahedron Lett.* **2000**, *41*, 359; (d) Kuwatani, Y.; Yoshida, T.; Kusaka, A.; Oda, M.; Hara, K.; Yoshida, M.; Matsuyama, H.; Iyoda, M. *Tetrahedron* **2001**, *57*, 3567; (e) Spitler, E. L.; Johnson, C. A., II; Haley, M. M. *Chem. Rev.* **2006**, *106*, 5344.
3. Yoshida, T.; Kuwatani, Y.; Hara, K.; Yoshida, M.; Matsuyama, H.; Iyoda, M.; Nagase, S. *Tetrahedron Lett.* **2001**, *42*, 53.
4. (a) Campbell, I. D.; Eglinton, G.; Henderson, W.; Raphael, R. A. *J. Chem. Soc., Chem. Commun.* **1966**, 87; (b) Staab, H. A.; Graf, F. *Tetrahedron Lett.* **1966**, 751; (c) Huynh, C.; Linstrumelle, G. *Tetrahedron* **1988**, *44*, 6337; (d) Solooki, D.; Ferrara, J. D.; Malaba, D.; Bradshaw, J. D.; Tessier, C. A.; Youngs, W. J. *Inorg. Synth.* **1997**, *31*, 122; (e) Iyoda, M.; Vorasingha, A.; Kuwatani, Y.; Yoshida, M. *Tetrahedron Lett.* **1998**, *39*, 4701; (f) Kehoe, J. M.; Kiley, J. H.; English, J. J.; Johnson, C. A.; Petersen, R. C.; Haley, M. M. *Org. Lett.* **2000**, *2*, 969; (g) Miljanic, O. S.; Vollhardt, K. P. C.; Whitener, G. D. *Synlett* **2003**, 29; (h) Iyoda, M.; Sirinintasak, S.; Nishiyama, Y.; Vorasingha, A.; Sultana, F.; Nakao, K.; Kuwatani, Y.; Matsuyama, H.; Yoshida, M.; Miyake, Y. *Synthesis* **2004**, 1527; (i) Li, Y.; Zhang, J.; Wang, W.; Miao, Q.; She, X.; Pan, X. *J. Org. Chem.* **2005**, *70*, 3285.
5. Staab, H. A.; Graf, F.; Doerner, K.; Nissen, A. *Chem. Ber.* **1971**, *104*, 1159.
6. (a) Sato, F.; Urabe, H.; Okamoto, S. *Chem. Rev.* **2000**, *100*, 2835; (b) Sato, F.; Urabe, H.; Okamoto, S. *Synlett* **2000**, 753.
7. All the new compounds reported here were fully characterized by spectroscopic methods and elemental analyses, see Supplementary data.
8. *Typical procedure for the synthesis of 2a from 3a*: To a solution of **3a** (250 mg, 0.83 mmol) in THF (58 ml) were added Ti(OPr^i)$_4$ (2.5 ml, 8.3 mmol) and Pr^{i}MgCl (9 ml of 2 M solution in diethylether, 18 mmol) at $-78\ ^\circ C$ under Ar atmosphere. The reaction mixture was stirred at $0\ ^\circ C$ for 2 h, and 2 M HCl (42 ml) was added to quench the reaction. The mixture was extracted with ether, and the combined organic layer was washed with satd aq NaHCO$_3$ solution and dried over anhydrous MgSO$_4$. After filtration, solvent was removed by evaporation. The residue was passed through a short column of Al$_2$O$_3$ using hexane–benzene (2:1) as an eluent and further purified by column chromatography on silica gel using hexane–benzene (4:1) as an eluent to give **2a** (210 mg, 83%).
9. Iyoda, M.; Fuchigami, K.; Kusaka, A.; Yoshida, T.; Yoshida, M.; Matsuyama, H.; Kuwatani, Y. *Chem. Lett.* **2000**, 860.
10. *X-ray analysis for 2a*: C$_{24}$H$_{16}$, MW = 304.39, monoclinic, $P2_1/a$ (#14), $Z = 4$, $a = 13.377(2)$ Å, $b = 12.2504(19)$ Å, $c = 10.6777(19)$ Å, $\beta = 109.456(14)^\circ$, $V = 1649.9(5)$ Å^3, $D_{calcd} = 1.225$ g cm^{-3}, $T = 298$ K, μ(Mo Kα) = 0.693 cm^{-1}, Rigaku AFC7R, Mo Kα ($\lambda = 0.71069$ Å), 246 parameters, $R_1 = 0.037$, $R_w = 0.114$, GOF = 1.000.
11. *X-ray analysis for 2b*: C$_{30}$H$_{28}$, MW = 388.55, prismatic, $Cmc2_1/a$ (#36), $Z = 4$, $a = 16.157(3)$ Å, $b = 8.8421(16)$ Å, $c = 15.956(3)$ Å, $V = 2279.5(7)$ Å^3, $D_{calcd} = 1.132$ g cm^{-3}, $T = 298$ K, μ(Mo Kα) = 0.635 cm^{-1}, Rigaku AFC7R, Mo Kα ($\lambda = 0.71069$ Å), 194 parameters, $R_1 = 0.034$, $R_w = 0.136$, GOF = 0.993. For the ORTEP drawing of **2b**, see Supplementary data.
12. *X-ray analysis for 2a·AgClO$_4$*: C$_{24}$H$_{16}$O$_4$ClAg, MW = 511.71, triclinic, $P\bar{1}$ (#2), $Z = 2$, $a = 10.821(3)$ Å, $b = 11.211(3)$ Å, $c = 9.2230(15)$ Å, $\alpha = 104.727(15)^\circ$, $\beta = 97.099(16)^\circ$, $\gamma = 67.428(18)^\circ$, $V = 998.8(4)$ Å^3, $D_{calcd} = 1.701$ g cm^{-3}, $T = 298$ K, μ(Mo Kα) = 11.692 cm^{-1}, Rigaku AFC7R, Mo Kα ($\lambda = 0.71069$ Å), 336 parameters, $R_1 = 0.052$, $R_w = 0.152$, GOF = 1.015.
13. *X-ray analysis for 2a·AgOTf*: C$_{25}$H$_{16}$O$_3$F$_3$SAg, MW = 561.32, triclinic, $P\bar{1}$ (#2), $Z = 2$, $a = 10.752(2)$ Å, $b = 12.225(2)$ Å, $c = 10.726(2)$ Å, $\alpha = 115.659(12)^\circ$, $\beta = 116.023(13)^\circ$, $\gamma = 67.732(13)^\circ$, $V = 1098.7(4)$ Å^3, $D_{calcd} = 1.697$ g cm^{-3}, $T = 298$ K, μ(Mo Kα) = 10.607 cm^{-1}, Rigaku AFC7R, Mo Kα ($\lambda = 0.71069$ Å), 349 parameters, $R_1 = 0.070$, $R_w = 0.181$, GOF = 1.070. For the ORTEP drawing of **2a·AgOTf**, see Supplementary data.
14. For the ^{1}H NMR data of **2c·AgOTf**, see Supplementary data.